A Diffusive Model for Halo Width Growth During VDEs

N.W. Eidietis and D.A. Humphreys

General Atomics, PO Box 845608, San Diego, California 92186-5608, USA

Email contact of main author: eidietis@fusion.gat.com

Abstract. The electromagnetic loads produced by halo currents during vertical displacement events (VDEs) impose stringent requirements on the strength of ITER in-vessel components. A predictive understanding of halo current evolution is essential for ensuring the robust design of those components. That evolution is primarily governed by three quantities: the resistivities of the core and halo regions, and the halo region width. A diffusive model of halo width growth during VDEs has been developed that provides one part of a physics basis for predictive halo current simulations. The diffusive model was motivated by DIII-D observations that VDEs with cold post-thermal quench plasma and a current decay time much faster than the vertical motion (Type I VDE) possess much wider halo region widths than warmer plasma VDEs where the current decay is much slower than the vertical motion (Type II). A 2-D finite element code is used to model current diffusion during selected Type I and Type II DIII-D VDEs. The model assumes a core plasma region within the last closed flux surface (LCFS) diffusing current into a halo plasma filling the vessel outside the LCFS. LCFS motion and plasma temperature are prescribed from experimental observations. The halo width evolution produced by this model compares favorably with the experimental measurements of Type I and Type II halo width evolution.

1. Introduction

Highly elongated tokamak discharges are inherently vertically unstable, and thus require active vertical control to maintain equilibrium [1]. If the vertical stabilization system fails, the plasma moves rapidly towards the top or bottom vessel wall in a vertical displacement event (VDE). Once the plasma limits upon the wall, its cross-section continues to compress against the wall. This compression, as well as L/R decay of the plasma current, drives significant open field line "halo" current in the plasma scrape-off layer (SOL). The halo current circuit includes both the plasma halo region and the vessel wall [2,3].

The electromagnetic loads produced by halo currents during VDEs impose stringent requirements on the strength of ITER vessel and in-vessel components [4,5], as well as those of future burning plasma devices. Those loads, directed perpendicular to the vessel wall, are produced by the interaction of the poloidal halo current and toroidal field. Since the detailed magnitude and spatial distribution of the halo current forces determine the constraints on in-vessel components, developing a predictive understanding of the halo current evolution is critical in order to ensure robust component design.

A simple 0-D halo current model can reliably reproduce the experimental evolution of bulk toroidal (I_{htor}) and poloidal (I_{hpol}) halo currents during a VDE [6]. However, a critical component of that 0-D model, or any model of halo current evolution, is the total resistance of the halo region. That resistance is primarily determined by the halo region resistivity η_h (in turn depending on electron temperature T_e and Z_{eff}) and width (w_h). In more complicated analyses, halo width is also important for calculating the distribution of poloidally localized forces upon in-vessel components. Unfortunately, no reliable physics basis exists for the prediction of η_h or w_h. Instead, values must be assumed from existing experiments.

The following sections present a 2-D model demonstrating that halo width growth can be described using only the basic principles of magnetic diffusion, reducing the unknowns for predictability to just one (η_h). Section 2 presents experimental observations of the wide variation in halo width evolution for different type of VDEs, and motivates the diffusive growth hypothesis. Section 3 describes the model implementation, and compares model results to experimental observation.

2. Experimental Evidence for Diffusive Halo Width Growth in DIII-D

Experimental evidence from the DIII-D tokamak [7] indicates that halo width evolves during a VDE, and that the details of the evolution vary significantly according to the type of VDE.

2.1 Diagnostic Methods

Three methods are used for diagnosing halo width evolution on DIII-D. The first, and least quantitative, is the plasma vertical position (z_p) estimator used by the real-time vertical control system. This signal is derived from a reduced set of magnetic probes and flux loops. The z_p estimator typically detects the expansion of the halo region as a reversal in the vertical velocity of the plasma current centroid (i.e. a "bounce") back towards the center of the vessel near the end of a VDE. While this signal does not provide quantitative information about the expansion of the halo region, it does qualitatively indicate the existence and timing of halo expansion for a given VDE.

The second method is the JFIT [6] diagnostic fitting code. This code calculates the distribution of poloidal flux and toroidal current within the vacuum vessel by inverting the Greens functions between a grid of distributed element plasma current sources and the magnetic diagnostics. After finding the last closed flux surface (LCFS), the distribution of core (inside the LCFS) and halo (outside LCFS) toroidal current is calculated, allowing for a quantitative measurement of halo width. Note that JFIT does not solve the Grad-Shafranov equation for a force-balanced equilibrium. However, fewer constraints enable JFIT to reliably converge during the fast transients of a VDE and to incorporate both closed and open field line currents into its reconstructions.

Finally, the Tile Current Array (TCA) [8] measures the flow of poloidal halo current into the DIII-D vessel floor. This diagnostic consists of a poloidally and toroidally distributed array of current shunts between electrically isolated graphite tile plasma facing components (PFCs) and the vessel wall. The TCA measures the poloidal halo current that travels from the plasma, through the tile, and into the vessel, as well as vice-versa.

2.2 VDE Classifications

VDEs may be characterized by the ratio of the current decay rate to the vertical decay rate [6]. In a "resistivity-dominated" or "Type I" VDE, the current decay rate is much more rapid than the vertical growth rate. In particular, I_p decreases faster than the compression of the plasma cross-section against the first wall, maintaining high edge q and generating relatively small poloidal halo currents (which are inversely proportional to edge q [6]). At the other extreme, the vertical growth rate dominates in a "motion-dominated", or "Type II", VDE, resulting in a slower rate of decrease of I_p relative to the shrinking plasma cross-

section. This typically produces an edge q approaching unity, resulting in higher poloidal halo current production. The Type I and Type II classifications represent the extrema of the possible spectrum of VDEs.

2.3. Experimental Data

Figure 1 displays a comparison of the halo width evolution of prototypical Type I and Type II VDEs. All traces begin at the time when the LCFS first limits upon the vessel floor (as measured using JFIT) and compression of the plasma cross-section begins. The core toroidal current is defined as the sum of reconstructed current within the LCFS. The sum of reconstructed current outside the LCFS defines the toroidal halo current. All quantities are calculated by JFIT. The halo width is calculated as current-weighted average distance from the LCFS:

$$w_{\mathrm{h}}(t) \equiv \frac{1}{I_{\mathrm{htor}}} \int_{A_{\mathrm{h}}} J_{\mathrm{htor}}(t)(r - r_{\mathrm{core}})\,dRdZ \qquad (1)$$

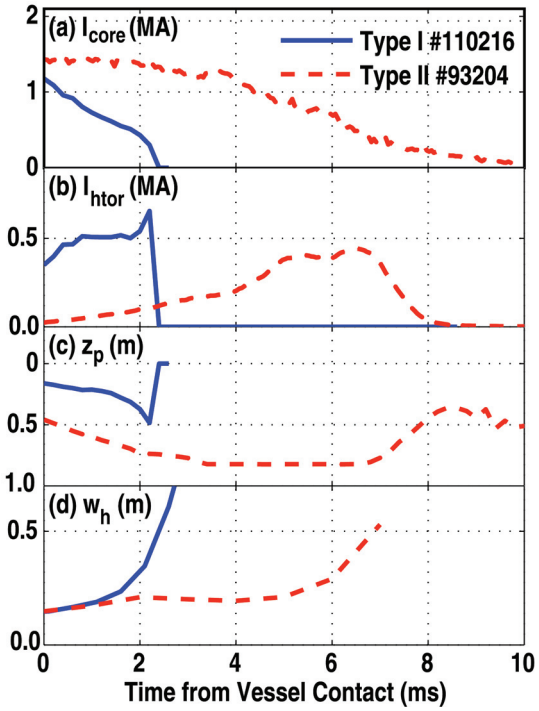

FIG. 1. Comparison of Type I & II VDE halo evolutions, as measured by JFIT: (a) core toroidal current, (b) halo region toroidal current, (c) toroidal current centroid vertical position (d) halo width.

where J_{htor} is the toroidal current density, r - r_{core} is the distance from the LCFS, and the halo region area A_{h} is the in-vessel region outside the LCFS.

Note that in the Type I case, I_{p} decays rapidly relative to the vertical position, whereas the Type II case retains the bulk of its I_{p} well into the compression period. Both z_{p} traces exhibit the characteristic "bounce" at the end of the VDEs, but the reversal of the Type I VDE occurs much earlier in the compression period than that of the Type II VDE. This is consistent with the much more rapid growth of the Type I halo width compared to that of the Type II, as displayed in Fig. 1(d).

Similar results are evident in the comparison of Type I and Type II TCA data. Figure 2 displays a comparison of Type I and Type II poloidal halo current profiles as measured on the floor of the vacuum vessel. The x-axis shows the distance from the LCFS of each TCA measurement tile poloidally along the floor. As shown in the figure, the Type I VDE possesses a wide, nearly flat poloidal halo current profile at the time of peak halo current. By contrast, the

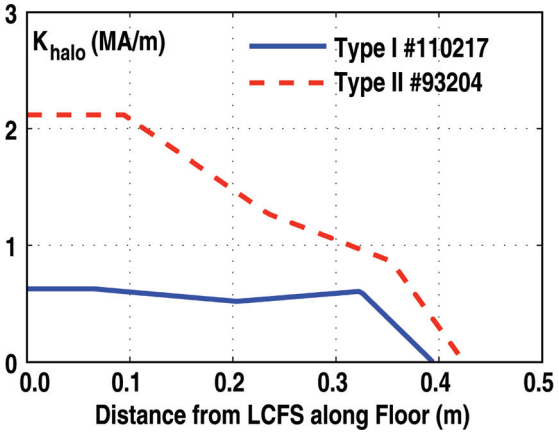

FIG. 2. TCA measurements of Type I & Type II VDE poloidal halo current distribution along floor of vessel at time of peak halo current.

Type II VDE halo current profile remains comparatively peaked, indicating a smaller current-weighted halo width.

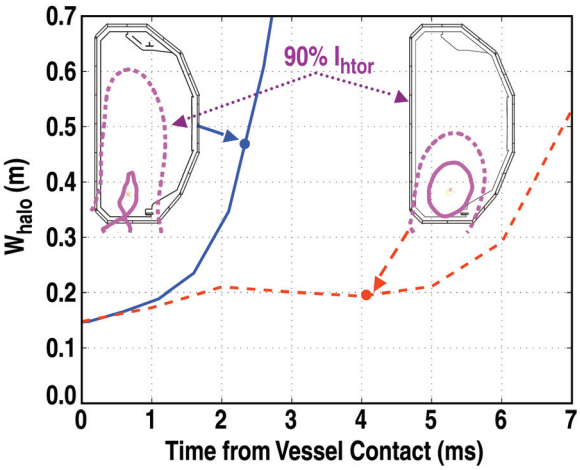

FIG. 3. Comparison of halo current distribution at approximately same point in vertical evolution of Type I and Type II VDEs. Dotted purple lines within vessel indicate flux surface encompassing 90% of toroidal halo current.

It should be noted that most of the halo width expansion is not isotropic. The bulk of the expansion is in the vertical direction, opposite the direction of VDE motion, rather than the much more constrained radial direction. This is made evident in Fig. 3, which displays a comparison of Type I and Type II VDE JFIT reconstructions superimposed upon the halo width data from Fig. 1(d). The reconstruction times are chosen to display the plasma core at approximately the same point in its vertical displacement. The flux contour that encompasses 90% of the toroidal halo current is shown for both reconstructions (dashed line). As this vertical expansion is not readily measured by in-wall current monitors, it may account for the relatively small difference in halo width visible in the direct tile current measurements [9].

2.4 Motivation for Diffusive Model of Halo Width Growth

The experimental data described above is qualitatively consistent with a halo width growth process governed primarily by magnetic diffusion of the form

$$\nabla^2 \mathbf{A} = -\frac{\mu_0}{\eta}\frac{\partial \mathbf{A}}{\partial t} \tag{2}$$

where **A** is the magnetic vector potential, η the plasma resistivity, and the term η/μ_0 is the magnetic diffusivity. Resistively dominated, cold Type I VDEs with corresponding cold halo regions would possess a high diffusivity, leading to rapid halo width growth. On the other hand, "warm" motion-dominated Type II VDEs with lower resistivity would possess less magnetic diffusivity, leading to slower halo width growth and thinner halo regions. This model assumes that a ubiquitous plasma exists outside the LCFS into which the core plasma can diffuse on a finite time-scale.

3. 2-D Diffusion Model of Halo Width Growth

3.1 Model Implementation

A 2-D finite element method (FEM) model has been developed to test the hypothesis of diffusive halo region growth. The model is implemented using the Comsol Multiphysics® FEM software and its ac/dc add-on module. It solves for the axisymmetric diffusion of the poloidal magnetic field (toroidal current) throughout the domains displayed in Fig. 4.

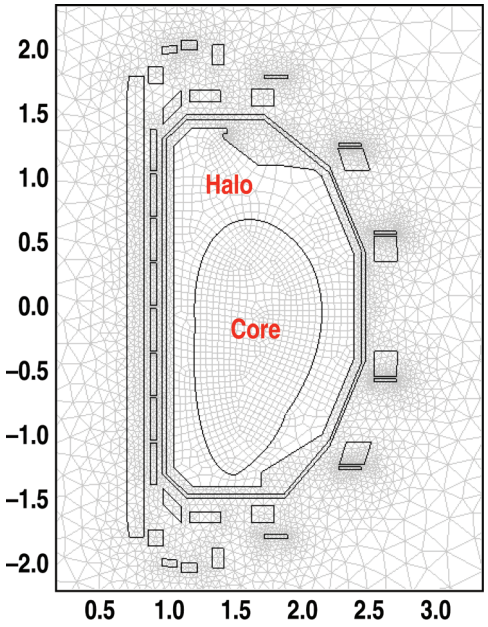

FIG. 4. Initial FEM model of Type I VDE #110216. Plasma domains are indicated.

The plasma region consists of two domains. The first is a core plasma domain of uniform T_e and initially uniform toroidal current density within the LCFS. It is surrounded by the halo domain, also of uniform T_e but initially no current, which fills the vessel outside the LCFS. The model not does calculate the core plasma motion using force balance consideration. Instead, the core domain motion during the VDE is prescribed to approximate experimental observations from JFIT. A deformable mesh algorithm adjusts the mesh to move with the core domain. The core and halo temperatures are derived from best fits to a 0-D halo current evolution model [9], and assumed to remain constant in time. The core and halo temperatures are prescribed to be 2 eV and 16 eV for the Type I and Type II VDEs, respectively. All coil currents are prescribed from experimental data.

The simulation begins at the point in time at which the plasma first limits upon the vessel floor, and FEM model calculates the diffusion of the toroidal vector potential (poloidal magnetic field or toroidal current) as the LCFS compresses against the vessel wall. The halo width can be calculated using Eq. (1) in order to allow a direct comparison between the empirical JFIT calculations and the model.

3.2 Results from 2-D Diffusion Model

The complete evolutions of the Type I and Type II VDE simulations are displayed in Fig. 5. The Type I and Type II are displayed in the left and right columns, respectively. Plots (a) and (b) display the toroidal core and halo current. These are followed by a time-evolving set of 2-D toroidal current distributions, with the time slice for each plot indicated by the associated dashed line in plots (a) and (b). The bottom plot displays toroidal current density cross-sections along the vertical dashed lines of the same color in the 2-D plots.

Figure 6 displays a comparison of the experimental halo width [from Fig. 1(d)] and that calculated from the simulations. The model exhibits good agreement with the qualitative features of the experimental halo width evolution. The Type I simulation exhibits a much more rapid growth rate than the Type II, as in experiment, and displays a similar late growth rate to the experiment. Similarly, the Type II simulation exhibits the same flattop in w_h between 2–4 ms as is seen in the experiment. However, the initial simulated growth rates far

exceed those of the experiment, leading to offsets between the model and experiments later in time.

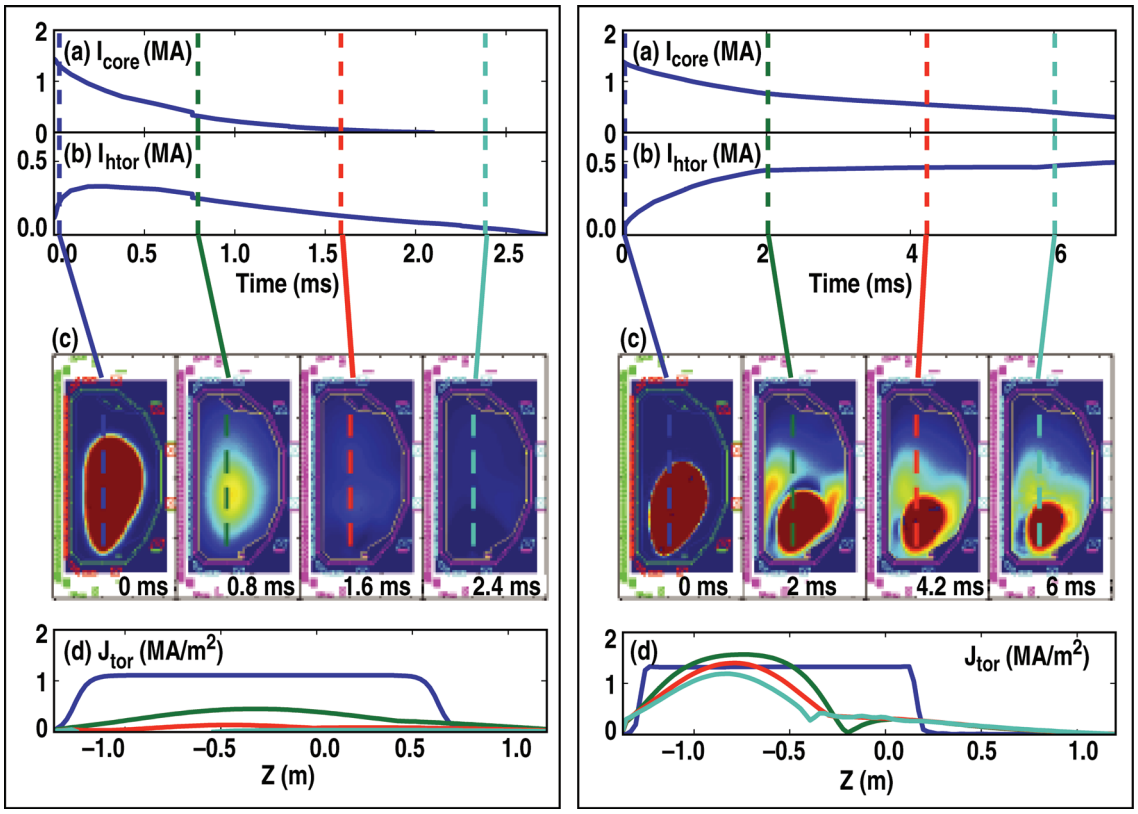

FIG. 5. Evolution of Type I (left) and Type II (right) simulations. (a) Core toroidal current (b) Toroidal halo current (c) J_{tor} within vessel (d) J_{tor} along dashed lines indicated in (c). Color bars of the same color indicate the same point in time.

There are numerous possible sources of this early discrepancy. Simplifying assumptions within the model, such as an initially uniform core current profile and static T_e, may play a role. The prescribed T_e, derived from a best fit of the 0-D halo current model described above to experiment, may also deviate from reality as a result of simplifying assumptions within the 0-D model. However, a parameter scan in T_e with the 2-D model indicates that the 0-D values (2 eV for Type I, 16 eV for Type II) provide the best agreement between the 2-D simulations and experiment as well.

The primary source of discrepancy is likely the model's lack of coupling to the diffusion of the poloidal current (toroidal field). Given the force-free constraint of a cold plasma (JxB=0), the toroidal current diffusion is strongly coupled to the poloidal current diffusion. Whereas the compression of the core plasma poloidal cross-section has only a secondary effect upon the direct induction of toroidal current, the resulting change in toroidal flux is the primary driver for poloidal current induction. Further inclusion of toroidal current driven by the poloidal current induction would likely retard the initial halo width growth. It would also provide a better match between simulated and experimental toroidal core current evolution.

4. Conclusions

Halo width is an important factor in determining total halo current evolution, and its growth rate can vary widely from one VDE to the next. A 2-D model of halo expansion has been developed based solely upon the principles of magnetic diffusion. This model compares favorably with experimental measurements of toroidal halo current width for both Type I and Type II VDEs, indicating that magnetic diffusion is indeed the dominant factor driving halo expansion. Detailed simulation codes may improve the accuracy of modeled halo width evolution during the current quench by allowing diffusion into a halo (open field line) plasma region that fills the entire vacuum vessel, but initially carries negligible current. Further model refinement includes coupling with the diffusion of poloidal current. Paired with a predictive model for halo resistivity, this work can provide a first principles physics basis for simulations of halo forces in ITER and future devices.

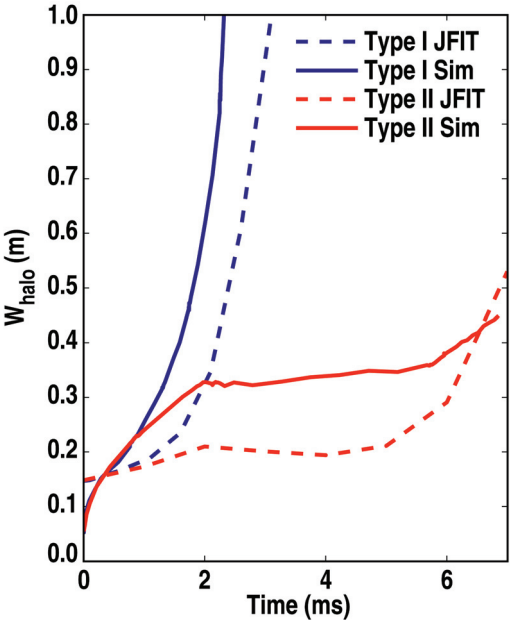

FIG. 6. Comparison of experimental and simulation halo width evolution.

This work was supported by the US Department of Energy under DE-FC02-04ER54698

References

[1] LAZARUS, E., *et al.,* "Control of the Vertical Instability in Tokamaks," Nucl. Fusion **30** (1990)

[2] JENSEN, T.H. and SKINNER, D.G., "Support of the Model for "Vertical Displacement Episodes" from Numerical Simulation of Episodes Observed in the DIII-D Tokamak," Phys. Fluids B **2** (1990) 2358

[3] STRAIT, E.J., *et al.,* Nucl. Fusion **31** (1991) 527

[4] HENDER, T.C., *et al.,* "Chapter 3: MHD Stability, Operational Limits and Disruptions," Nucl. Fusion **47** (2007) S128

[5] SUGIHARA, M., *et al.,* "Disruption Scenarios, Their Mitigation and Operation Window in ITER," Nucl. Fusion **47** (2007) 337

[6] HUMPHREYS, D.A., and KELLMAN, A.G., "Analytic Modeling of Axisymmetric Disruption Halo Currents," Phys. Plasmas **6** (1999) 2742

[7] LUXON, J.L., "A Design Retrospective of the DIII-D Tokamak," Nucl. Fusion **42** (2002) 614

[8] EVANS, T.E., *et al.,* "Measurements of Non-axisymmetric Halo Currents With and Without "Killer" Pellets During Disruptions in the DIII-D Tokamak," J. Nucl. Mater. **241-243** (1997) 606

[9] HUMPHREYS, D.A, *et al.,* "Predictive Modeling of Plasma Halo Evolution in Post-Thermal Quench Disrupting Plasmas," Proc. 33rd EPS Conference on Controlled Fusion and Plasma Physics, Rome, Italy (2006)